Figure S1 De Franceschi et al.

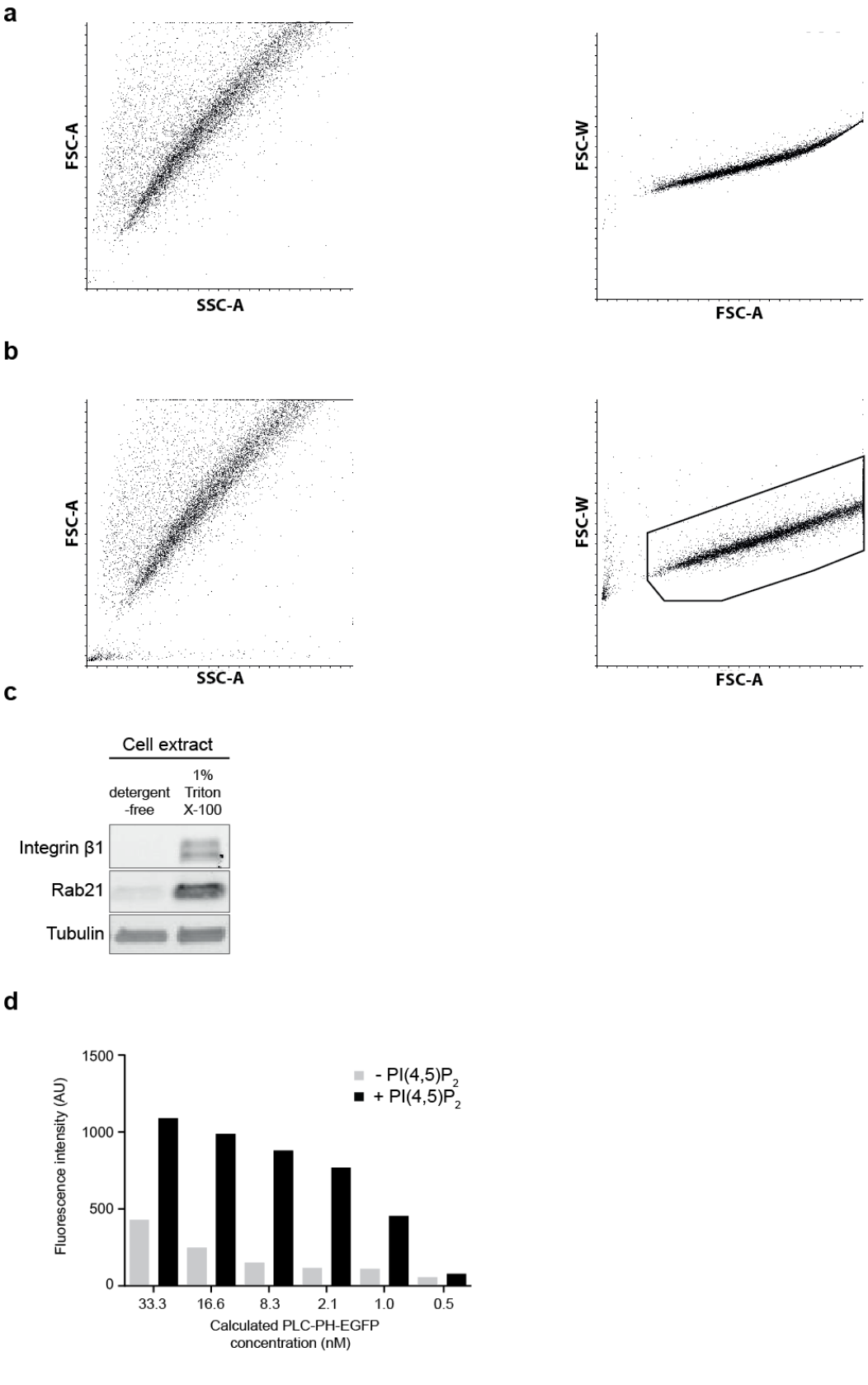

Supplementary Figure 1

a: Detection of SA-beads by flow cytometry. 1/1000 of the events typically detected in one sample are shown.

b: Scatter plots resulting from biotinylated-liposomes bound to SA-beads by flow cytometry. 1/1000 of the events typically detected in one sample are shown.

c: Western blot analysis of the isolated detergent-free cell lysate fraction used in liposome binding assays compared to the Triton X-100-solubilized fraction rich in transmembrane (β1 integrin) and membrane associated proteins (Rab21). Uncropped blots can be found in Figure S6.

d: Titration curve with decreasing amounts of PLC-PH-EGFP (n = 1). Cell lysates from PLC-PH-EGFP transfected cells were diluted to contain the indicated concentrations of the protein (calculated based on equation (1)), incubated with liposomes with and without $PI(4,5)P_2$ and analyzed for protein-liposome binding using FACS.

Figure S2 De Franceschi et al.

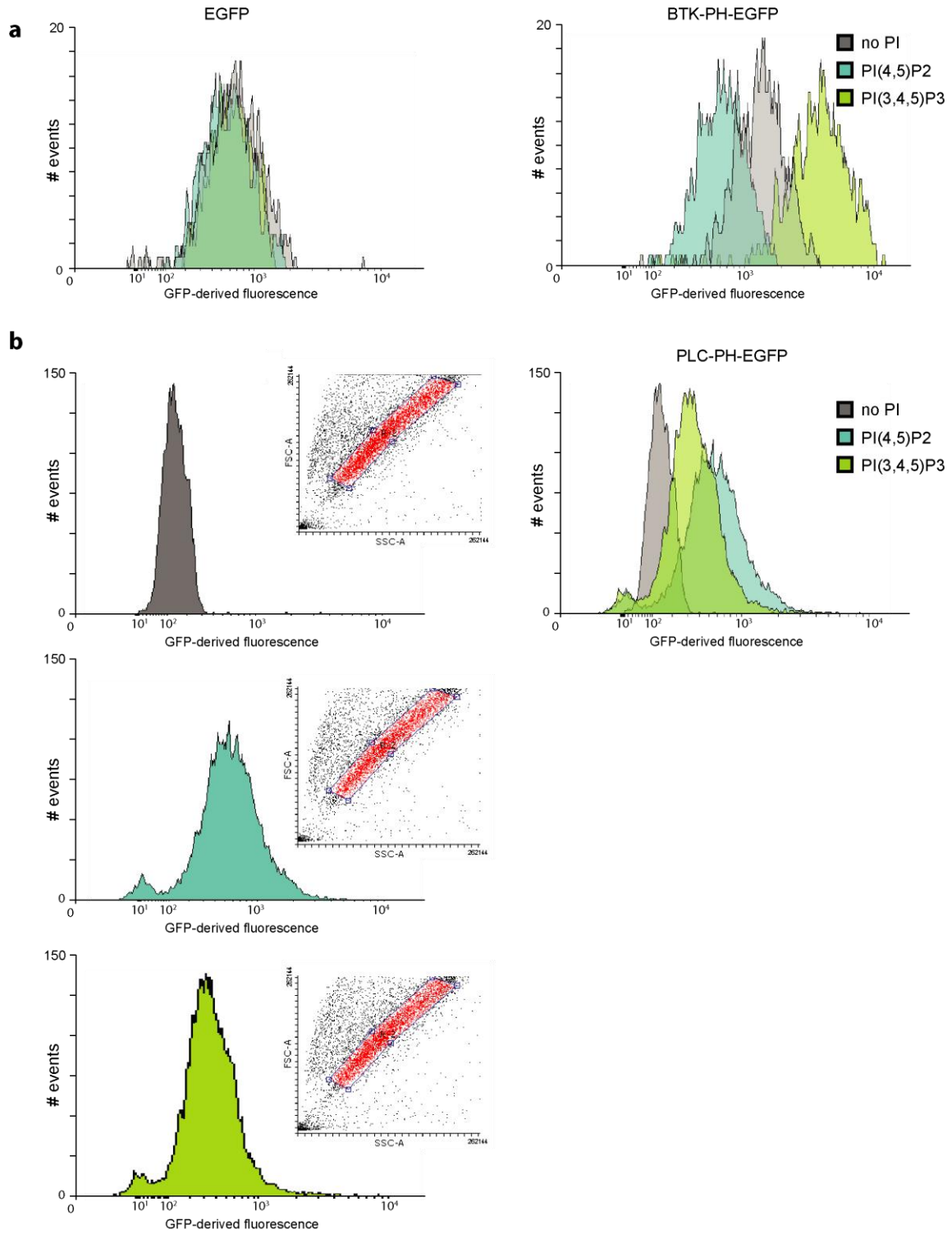

Supplementary Figure 2

a: Overlay of fluorescence intensity histograms of EGFP and BTK-PH-EGFP bound to different PI species (individual histograms shown in Fig. 1d).

b: Representative scatter plots, fluorescence intensity histograms and histogram overlays (from experiments quantified in Fig. 1f) of PLC-PH-EGFP bound to different PI species. The red population in the scatter plot was gated for quantification.

Figure S3 De Franceschi et al.

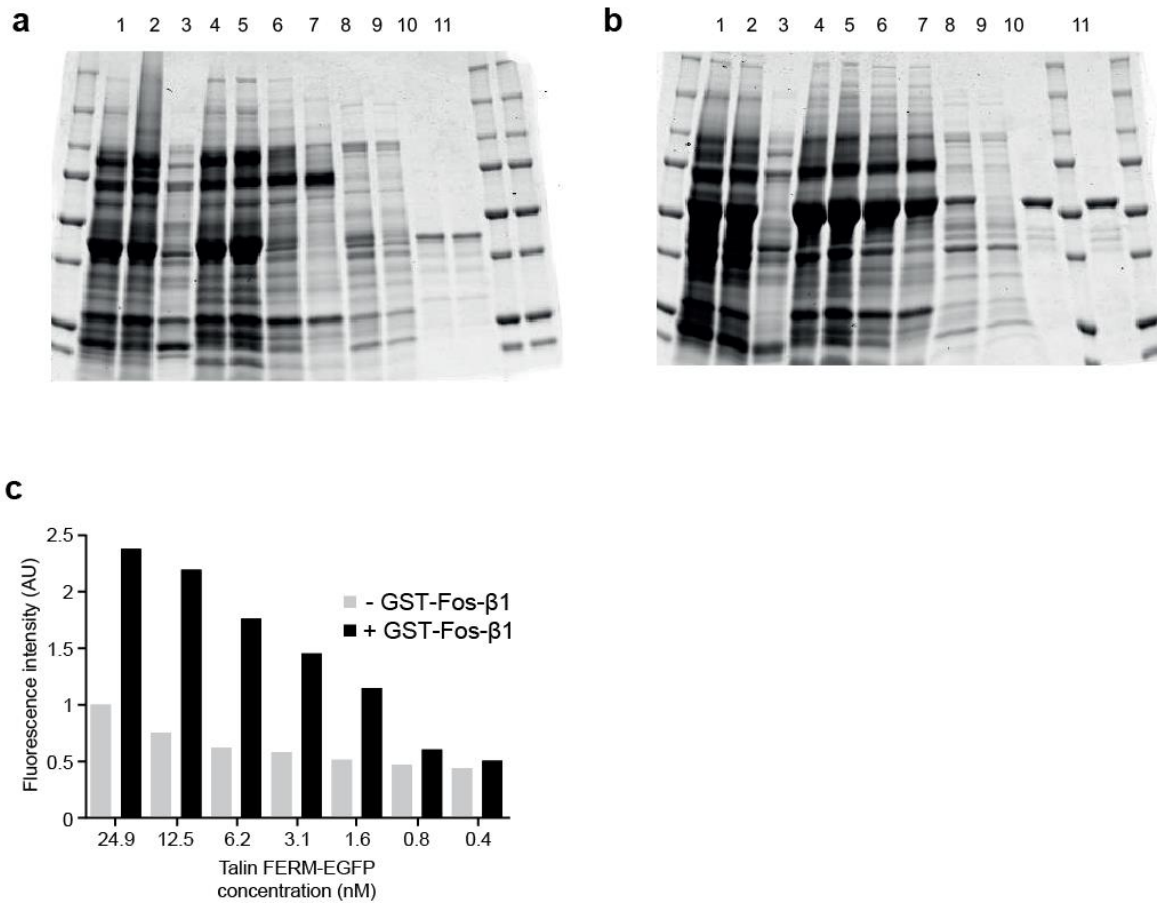

Supplementary Figure 3

a,b: Sequential steps in GST-Fos-β1 (a) and MBP-Jun-α5 (b) purification. Shown are coomassie-stained SDS-PAGE gels loaded with the following samples: #1, whole lysate after cell disruption; #2, supernatant from low-speed centrifugation; #3, supernatant from high-speed centrifugation; #4, resuspended membrane pellet from high-speed centrifugation; #5, resuspended membrane pellet after solubilisation in DDM; #6 supernatant from high-speed centrifugation; #7, flow-through from Ni2+ matrix; #8, eluted from Ni2+ matrix; #9, flow-through from glutathione or amylose matrix; #10, eluted from glutathione or amylose matrix; #11, protein stored after dialysis.

c: Titration curve with decreasing amount of Talin FERM-EGFP (n = 1). Cell lysates from Talin FERM-EGFP transfected cells were diluted to contain the indicated concentrations of the protein (calculated using equation (1)), incubated with liposomes with and without GST-Fos-β1 and analyzed for protein-liposome binding using flow cytometry.

Figure S4 De Franceschi et al.

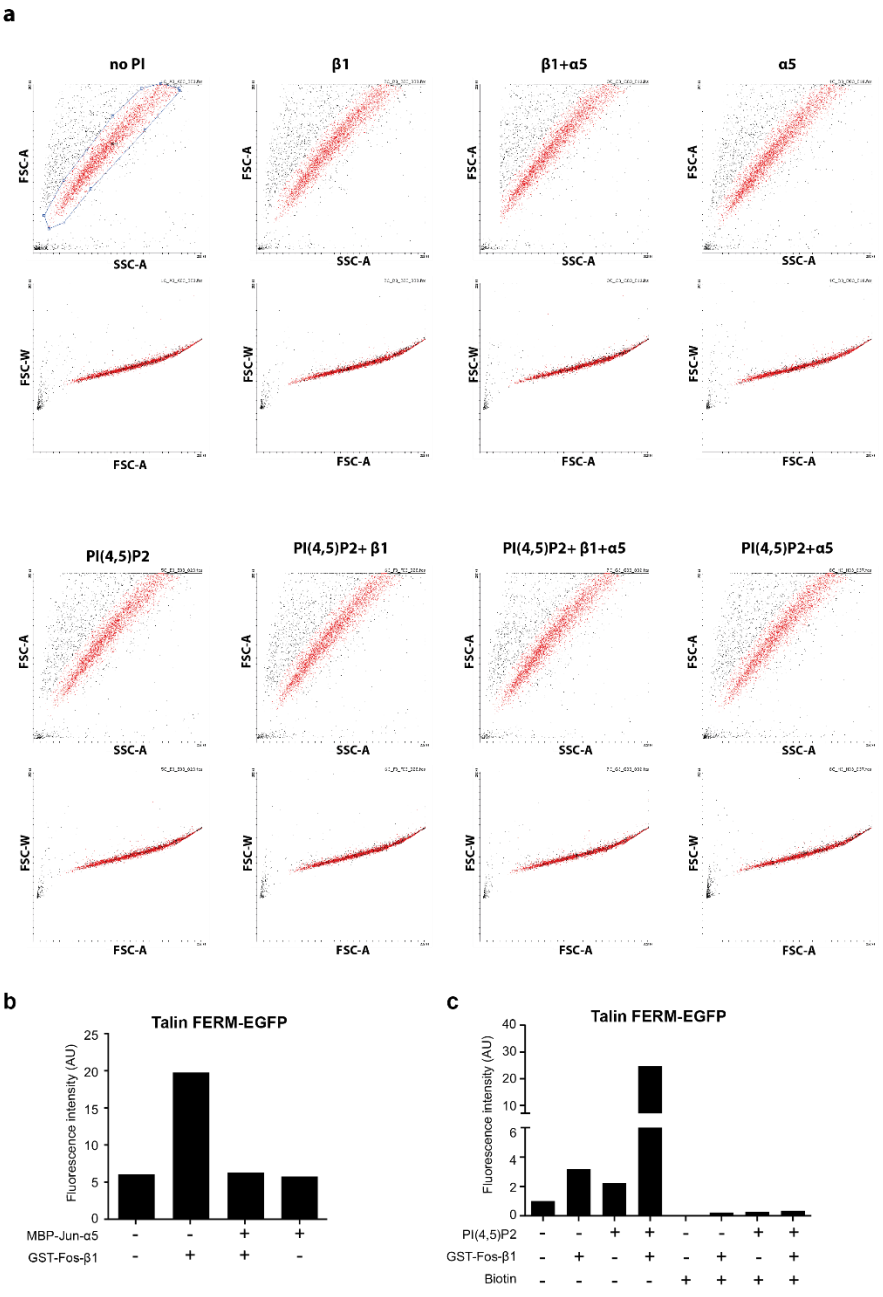

Supplementary Figure 4

a: Representative flow cytometry FSC-A vs SSC-A and FSC-A vs FSC-W scatter plots of SA-beads for all Talin FERM-EGFP samples shown in Fig.4b. The red population was gated for quantification.

b: ProLIF assay monitoring Talin FERM-EGFP (3nM; cell lysate) binding to proteoliposomes containing GST-Fos-β1 and/or MBP-Jun-α5 at a lower (compared to Fig. 4b) protein:lipid molar ratio of 1:7000 (n = 1).

c: Competition of Talin FERM-EGFP binding to proteoliposomes by addition of soluble biotin. Biotinylated-lipid-containing liposomes (containing GST-Fos-β1 and $PI(4,5)P_2$ as indicated) were incubated with Talin FERM-EGFP-containing cell lysate and captured on SA-beads in the presence or absence of free biotin and analyzed using FACS. Molar ratio between biotinylated lipids and soluble biotin is 1:50 (n = 1).